Molecular Phylogenetics and Evolution 68 (2013) 81–92

Contents lists available at SciVerse ScienceDirect

Molecular Phylogenetics and Evolution

journal homepage: www.elsevier.com/locate/ympev

Molecular phylogeny, divergence times and biogeography of spiders of the subfamily Euophryinae (Araneae: Salticidae)

Jun-Xia Zhang [a,*], Wayne P. Maddison [a,b]

[a] Department of Zoology, University of British Columbia, Vancouver, BC, Canada V6T 1Z4
[b] Department of Botany and Beaty Biodiversity Museum, University of British Columbia, Vancouver, BC, Canada V6T 1Z4

ARTICLE INFO

Article history:
Received 10 August 2012
Revised 17 February 2013
Accepted 13 March 2013
Available online 28 March 2013

Keywords:
Phylogeny
Temporal divergence
Biogeography
Intercontinental dispersal
Euophryinae
Diolenius

ABSTRACT

We investigate phylogenetic relationships of the jumping spider subfamily Euophryinae, diverse in species and genera in both the Old World and New World. DNA sequence data of four gene regions (nuclear: 28S, Actin 5C; mitochondrial: 16S-ND1, COI) were collected from 263 jumping spider species. The molecular phylogeny obtained by Bayesian, likelihood and parsimony methods strongly supports the monophyly of a Euophryinae re-delimited to include 85 genera. *Diolenius* and its relatives are shown to be euophryines. Euophryines from different continental regions generally form separate clades on the phylogeny, with few cases of mixture. Known fossils of jumping spiders were used to calibrate a divergence time analysis, which suggests most divergences of euophryines were after the Eocene. Given the divergence times, several intercontinental dispersal events are required to explain the distribution of euophryines. Early transitions of continental distribution between the Old and New World may have been facilitated by the Antarctic land bridge, which euophryines may have been uniquely able to exploit because of their apparent cold tolerance. Two hot-spots of diversity of euophryines are discovered: New Guinea and the Caribbean Islands. Implications of the molecular phylogeny on the taxonomy of euophryines, and on the evolution of unusual genitalic forms and myrmecophagy, are also briefly discussed.

1. Introduction

The subfamily Euophryinae as here delimited is a major clade of Salticidae (jumping spiders) with about 1000 described species (Platnick, 2012; Zhang and Maddison, 2012a,b,c,d). It belongs to the Salticoida, a lineage comprising the vast majority of jumping spider species (Maddison and Hedin, 2003a).

Initially erected by Eugène Simon (1901) using the name "Evophrydeae", the subfamily Euophryinae received its first modern delimitation by Jerzy Prószyński (1976), who characterized it by the presence of a coiled embolus at the distal end of the palpal tegulum. This delimitation was further revised by Maddison and Hedin (2003a) to clarify the specific genitalic forms of euophryines. Maddison and Hedin (2003a) also considerably extended the content of Euophryinae and listed 34 genera as members of the subfamily, which makes Euophryinae one of the largest groups in jumping spiders. To date, twelve euophryine genera have been sampled in molecular phylogenetic studies of jumping spiders, and the monophyly of Euophryinae has been supported (Maddison and Hedin, 2003a; Maddison et al., 2008; Bodner and Maddison, 2012). However, many other potential euophryine genera are unstudied, and the phylogenetic relationships within the Euophryinae are still poorly understood (see Bodner, 2002).

The Euophryinae has remained the largest biogeographically unresolved group of salticid spiders. Most major salticid clades are primarily restricted to one continental region, with few or no representatives in the other (Maddison and Hedin, 2003a; Maddison et al., 2008; Bodner and Maddison, 2012). This has suggested that most salticid radiations post-date continental separation, and that intercontinental dispersals have been limited (Bodner and Maddison, 2012). The Euophryinae is the one remaining group that could be an exception to this pattern, being phylogenetically unresolved and well represented in both the Old World and New World. Among the 85 currently recognized genera (see discussion), 54 are mainly from the Old World and 31 are from the New World. If the phylogeny resolves with Old and New World euophryines mixed thoroughly, then it would suggest that euophryines have undergone unusually many intercontinental dispersals, or that their radiation is older than that of most other salticid groups. These possibilities can be tested by a dated molecular phylogeny.

In this study, we collected molecular data from an extensive sampling of euophryine taxa to test if all or most of euophryines are a monophyletic group, to resolve the phylogenetic

* Corresponding author. Address: Department of Zoology, 6270 University Boulevard, University of British Columbia, Vancouver, BC, Canada V6T 1Z4. Fax: +1 604 822 2416.
E-mail address: jxzhang1976@gmail.com (J.-X. Zhang).

1055-7903/$ - see front matter © 2013 Elsevier Inc. All rights reserved.
http://dx.doi.org/10.1016/j.ympev.2013.03.017

relationships within the Euophryinae, and to reveal the continental distribution pattern of euophryine clades. We also took advantage of the molecular phylogeny with worldwide sampling to explore the temporal evolution of this subfamily calibrated by fossil records of salticids. Implications of the divergence times on biogeography are discussed. Insights from the molecular phylogeny on euophryine classification and on the evolution of unusual genitalic forms and myrmecophagy are briefly introduced.

2. Material and methods

2.1. Taxon sampling

In total, we collected molecular data from 263 jumping spider species, most of them euophryine or potential euophryine species, with the sampling covering all areas of euophryine biodiversity: Eurasia, Africa, Australasia, North America, Central and South America, and the Caribbean Islands. *Diolenius* and its relatives, and *Bristowia* were also included because their position on the jumping spider phylogeny had been a mystery (Maddison and Hedin, 2003a; Maddison et al., 2008). In addition, sequences of 28 salticid species were obtained from previous studies (Maddison and Hedin, 2003a,b; Maddison and Needham, 2006; Maddison et al., 2008; Bodner and Maddison, 2012) to represent all other major groups of jumping spiders. One thomisid species was also included to represent an outgroup of Salticidae.

A full list of species included in this study with collection localities, gene information and GenBank accession numbers is given in Appendix A. All voucher specimens are preserved in 95% ethanol and stored at −20 °C, and deposited in the Spencer Entomological Collection at the Beaty Biodiversity Museum, University of British Columbia.

2.2. DNA extraction, PCR amplification and sequencing

For total genomic DNA extraction, usually legs were used. For small specimens, cephalothorax (female) or abdomen (male) or the whole body except genitalia was used to obtain enough amount of total genomic DNA for gene amplification. The rest of each specimen was kept as a voucher. The Puregene DNA Purification Kit (Gentra Systems) was used for total genomic DNA extraction.

Four gene regions were amplified and sequenced for phylogenetic analyses: the nuclear 28S and Actin 5C, and the mitochondrial 16S-ND1 and COI. Most sequences were amplified and sequenced with primers that have been widely used in jumping spider molecular phylogenetic studies (Maddison and Hedin, 2003a,b; Maddison and Needham, 2006; Maddison et al., 2007, 2008; Bodner and Maddison, 2012). However, about 30% of 16S-ND1 sequences could not be amplified by the commonly used primers. For these, two pairs of internal primers (16SND1-WPM-F1/R3 and 16SND1-WPM-F2/R2) were designed and proved to be successful. Three pairs of internal primers (28S-WPM-F1, F2, F3/28S-WPM-R1, R2, R3) were also designed to amplify or sequence a small number of difficult 28S fragments. A summary of all primers used in this study is shown in Appendix B (also see Simon et al., 1994; van der Auwera et al., 1994; Hedin, 1997; Hedin and Maddison, 2001).

The polymerase chain reaction (PCR) was run using either Paq5000 DNA Polymerase (Agilent Technologies) or Taq DNA Polymerase (Invitrogen), with their respective buffers, the dNTPs supplied by Invitrogen and the primers supplied by Oligo. The PCR conditions to amplify 28S, Actin 5C and COI were as follows (using Paq5000 DNA Polymerase): initial denaturation at 95 °C for 2 min; 35 cycles of 45 s at 95 °C, 45 s of annealing at 52–62 °C (28S), 55–57 °C (Actin 5C) or 45–50 °C (COI), 1 min at 72 °C; followed by a 10 min extension at 72 °C. The PCR conditions to amplify 16S-ND1 were (using Paq5000 DNA Polymerase): initial denaturation at 94 °C for 2 min; 35 cycles of 35 s at 94 °C, 35 s of annealing at 44–55 °C, 70 s at 65 °C; followed by a 10 min extension at 65 °C (Maddison and Hedin, 2003a,b; Maddison and Needham, 2006; Maddison et al., 2008; Bodner and Maddison, 2012). In general, when Taq DNA Polymerase was used the annealing temperature usually had to be decreased 4–10 °C.

Sequencing reactions were usually conducted with the pair of primers used for PCR. About half of the PCR products were sent to Macrogen Inc. (Korea) and sequenced with the 3730xl DNA analyzer. All other PCR products were purified with the QIAquick PCR purification Kit (QIAGEN Inc.), and then were sent to the University of British Columbia NAPS facility and sequenced on the Applied Biosystems 3730 DNA Analyzer.

The chromaseq package (Maddison and Maddison, 2010b) for Mesquite (Maddison and Maddison, 2010a) was used to obtain sequences from chromatograms by Phred (Ewing and Green, 1998; Ewing et al., 1998; Green and Ewing, 2002) and Phrap (Green, 1999), and to further proofread the sequences by comparing against the chromatograms (Maddison and Needham, 2006).

In total, 938 sequences (259 of 28SrDNA, 255 of Actin 5C, 258 of 16S-ND1 and 166 of COI) from 263 jumping spider species were amplified and sequenced, and combined with 106 sequences obtained from previous work (Maddison and Hedin, 2003a,b; Maddison and Needham, 2006; Maddison et al., 2008; Bodner and Maddison, 2012).

2.3. Sequence alignment

To find the boundary of the intron region, Actin 5C sequences were aligned with the cDNA sequence of *Paraphidippus aurantius* (Lucas) (GeneBank Accession No. EU293228; see Vink et al., 2008). The introns were highly variable and very difficult to align, and thus excluded from analyses (Vink et al., 2008). To find the boundary of ND1 within the 16S-ND1 region, we used amino acid translation in comparison with ND1 sequences of *Habronattus oregonensis* (Peckham & Peckham) from the complete mitochondrial genome (GeneBank Accession No. AY571145; see Masta and Boore, 2004). The protein-coding data (Actin 5C exon region, ND1 and COI) were then manually aligned in Mesquite (Maddison and Maddison, 2010a) with reference to the amino acid translation using the "Color Nucleotide by Amino Acid" option.

For regions other than protein-coding, Opal (Wheeler and Kececioglu, 2007) run via Mesquite 2.73 (Maddison and Maddison, 2010a) was used for alignment. Opal was chosen after preliminary alignments in both CLUSTALW (Larkin et al., 2007) and Opal were attempted. The CLUSTALW alignments showed many obvious misalignments, but Opal alignments showed only a few visible misalignments. Furthermore, we explored the performance of ten combinations of gap open/gap extension costs in Opal (200/100, 260/69 [default], 300/100, 300/200, 400/100, 400/200, 400/300, 500/300, 600/200, 800/200) for alignment of 28S and 16S (plus the adjacent tRNA). The preliminary ML searches on different alignments and the concatenation of all alignments were conducted using GARLI0.96b8 (Zwickl, 2006) with five search replicates and the GTR invariant-gamma model (GTR + I + G). Apparent misalignments were recognized by the "Highlight Apparently Slightly Misaligned Regions" tool and manually edited in Mesquite. The ten different gap open/gap extension costs resulted in distinct 28S + 16S alignments with the aligned lengths ranging from 2018 to 2287 bp and the parsimony-informative sites ranging from 1055 to 1119 bp. The phylogenetic tree from the "260/69" alignment was most topologically congruent with that from the concatenated alignments. Thus, the elision matrix approach (Wheeler

et al., 1995) supports the choice of defaults in Opal, which Wheeler and Kececioglu made on the basis of careful study of performance of different settings (T. J. Wheeler, pers. comm.). Thus we utilized the "260/69" alignments for more comprehensive analyses.

2.4. Phylogenetic reconstruction

Phylogenetic analyses were performed on the individual gene matrices (28S, Actin 5C, 16S-ND1 and COI) and a combined matrix with all genes concatenated. In the combined matrix, the data were further divided into eight partitions: 28S; Actin 5C first, second and third codon positions; 16S; ND1 + COI first, second and third codon positions.

2.4.1. Model selection

Modeltest 3.7 (Posada and Crandall, 1998; Posada and Buckley, 2004) in combination with PAUP* 4.0b10 (Swofford, 2002) was used to choose the appropriate substitution model for each dataset and each partition via the Akaike Information Criterion (AIC). Most of the datasets had the GTR + I + G as the best-fit model. However, for the individual gene matrices "Actin 5C" and "16S-ND1", the TVM + I + G model was chosen, and for the partitions in the combined matrix, HKY + G was chosen for the "Actin 5C 2nd codon position" partition, K81uf + I + G was chosen for the "16S" partition, and TVM + G was chosen for the "ND1 + COI 3rd codon position" partition.

2.4.2. Maximum likelihood (ML) analysis

GARLI0.96b8 (Zwickl, 2006) was used to perform maximum likelihood analyses on the individual gene matrices, each with 100 search replicates. All the settings were defaults except the model was specified as that chosen in Modeltest. The model parameters were optimized during the tree-searching process. Bootstrap analyses were also carried out to calculate the replicability of clades in a separate GARLI run with 500 bootstrap replicates.

For the combined matrix, a test version of GARLI (GARLI-partition-r601, https://www.nescent.org/wg_garli/Partition_testing_version) was used for the maximum likelihood tree search to allow each partition to have its own model or model parameters. The four GARLI search parameters (topoweight, modweight, brlenweight, scorethreshforterm) were set to 0.05, 0.009, 0.002, 0.001 respectively. Five hundreds search replicates were carried out to find the best ML tree. Because the GARLI run on the combined matrix with eight partitions took about 30 h to complete each search replicate, it would have been too time expensive to do an extensive bootstrap analysis using GARLI. Instead, 1000 replicates of bootstrap analysis on the combined matrix were completed in RAxML 7.0.4 (Stamatakis, 2006; Stamatakis et al., 2008) with a GTRCAT model for each partition and model parameters permitted to differ among data partitions (command line as "./raxmlHPC -f d -# 1000 -b 3 -s CombinedMatrixW30OutPartition.phy -n 1000 boots.out -q partition -m GTRCAT").

2.4.3. Bayesian (BI) analysis

MrBayes v. 3.1.2 (Huelsenbeck and Ronquist, 2001; Ronquist and Huelsenbeck, 2003; Altekar et al., 2004) was used to perform a Bayesian analysis on the combined matrix with the data divided into eight partitions (28S; Actin 5C first, second and third codon positions; 16S; ND1 + COI first, second and third codon positions). Each partition was allowed to use the model selected by Modeltest. In case that the model selected by Modeltest was not implemented in MrBayes, the next more complex model available in the program was used instead. The analysis was run using the following parameters: mcmcp ngen = 200,000,000 printfreq = 1000 samplefreq = 1000 nchains = 8 savebrlens = yes. However, it was terminated at 120,000,000 generations as the stdDev of clade frequencies already reached 0.007. Trees that were sampled before the likelihood had stabilized were discarded as "burn-in". The remaining trees from these two runs were collected and input for the majority rule consensus using PAUP* 4.0b10 (Swofford, 2002) to count the frequency of various clades.

2.4.4. Maximum parsimony (MP) analysis

MP analyses were conducted on the individual gene matrices and the combined matrix. TNT 1.1 (Goloboff et al., 2008) was run to find most parsimonious trees using "New Technology Search" method with default settings except (1) sectorial search with XSS, CSS and RSS all selected; (2) rachet and drift selected with default settings; (3) tree fusing with "Do global fuse every 2 hits" and "Dump fused trees to prevent clogging" selected; (4) the option to find the minimum length 20 times for all the matrices except for Actin 5C (set to find the minimum length 50 times instead). To find more equally parsimonious trees, the trees found by TNT were imported into PAUP* 4.0b10 (Swofford, 2002) and swapped on using tree bisection reconnection (TBR) branch swapping without constraint except by MAXTREES of 1,000,000. The strict consensus tree of all the equally most parsimonious trees was built in PAUP.

2.5. Divergence time analyses

Divergence time analyses were conducted on the combined all genes matrix in which 262 euophryine sequences and 30 outgroup sequences were included. Three *Athamas* species were not included in this matrix for reasons discussed below with the 28S results.

2.5.1. Calibrations

Four calibration points were chosen based on fossil records of spiders. The first three are following Bodner and Maddison (2012): (1) age of the most recent common ancestor of the Salticidae (minimum 44 Ma based on oldest fossil salticid, Baltic Amber; maximum 100 Ma based on absence in Cretaceous amber), (2) age of the most recent common ancestor of the Salticoida (minimum 16 Ma based on oldest fossil Salticoida, Dominican Amber; maximum 49 Ma based on absence in Baltic Amber), (3) age of the Lyssomaninae/Spartaeinae divergence (minimum 22 Ma based on oldest fossil *Lyssomanes*, Chiapas Amber; maximum 100 Ma based on absence of salticids in Cretaceous amber). The fourth calibration point, the age of the divergence of Euophryinae and its sister group, is new to this study.

The fourth of these calibration points is based on euophryine fossils. Six euophryine fossil species have been reported from the Dominican Republic amber: *Corythalia ocululiter*; *C. pilosa*; *C. scissa*; *Pensacolatus coxalis*; *P. spinipes*; *P. tibialis* (see Penney, 2008). The holotypes of *Pensacolatus coxalis* (SMF Be 938) and *P. spinipes* (SMF Be 930) were borrowed from the Research Institute and Natural History Museum Senckenberg (Germany). These two species are confirmed to be euophryines based on the typical palp structure. However, all features noticed in the fossil species are either ancestral or multiply derived. Clear synapomorphies that could place them within euophryine clades are either invisible or absent in the fossil specimens. Thus, they cannot be confidently placed in any clade within euophryines. For this reason, the calibration point supplied by the Dominican amber euophryines was put at the base of split between Euophryinae and its sister group. As the Dominican Republic amber is estimated to be 16 Ma (Penney, 2008), we therefore set the minimum age of the Euophryinae/Sister-group node at 16 Ma. No euophryine fossil species has been discovered in earlier deposits, including the Baltic amber (estimated to be 49 Ma (Weitschat and Wichard, 2002 as cited in Penney, 2008)). We therefore set the node's maximum age at 49 Ma.

The maximum constraints on two of the calibration points, Salticoida and Euophryinae/Sister-group, are based on the absence of fossils of these groups in Baltic amber. It could be argued that salticoids and euophryines may be much older, but simply absent

from the Baltic fauna (see discussion in Bodner and Maddison, 2012). Therefore, to be conservative, we also ran an independent analysis with the maximum constraints of the Salticoida and the Euophryinae/Sister-group loosened (set to 100 Ma instead of 49 Ma). A summary of the two sets of constraints in the divergence time analyses is given in Table 1.

2.5.2. Bayesian analysis using BEAST

Divergence times were estimated by Bayesian MCMC using BEAST v1.5.3 (Drummond and Rambaut, 2007). BEAUti v1.5.3 (Drummond and Rambaut, 2007) was used to generate a BEAST XML file. The dataset was also divided into eight partitions (28S; Actin 5C first, second and third codon positions; 16S; ND1 + COI first, second and third codon positions). The model assignment for each partition was the same as in the MrBayes analysis. Four MRCA (most recent common ancestor) groups were established: Salticidae, Salticoida, Lyssomaninae/Spartaeinae, Euophryinae/Sister-group, with none of them restricted to be monophyletic. The upper and lower constraints of the calibration points (see Table 1 for details of the two sets of constraints) were specified as tMRCA (time to most recent common ancestor) prior to estimating the age of divergence using the relaxed (uncorrelated lognormal) molecular clock model. The best tree found by a preliminary ML search using GARLI0.96b8 (five search replicates and GTR + I + G model) was modified into an ultrametric tree in Mesquite (Maddison and Maddison, 2010a) and used as the starting tree for the BEAST analysis. Analysis under each set of constraint was run for 200,000,000 generations (trees sampled at every 1000 generations). Tracer v1.5 (Rambaut and Drummond, 2007) was used to check when the MCMC chains had reached a stationary distribution by visual inspection of plotted posterior estimates, and by checking that ESS (Effective Sample Size) was greater than 200 for all parameters. Using the LogCombiner v1.5.3 program (Drummond and Rambaut, 2007), trees sampled during the first 50,000,000 generations (25%) were removed as burn-in and the remaining trees were resampled at lower frequency (every 2000 generations) to generate a smaller tree file for annotation. These trees resampled from the BEAST analyses were summarized on the best ML tree from the GARLI all-genes partitioned analysis in TreeAnnotator v1.5.3 (Drummond and Rambaut, 2007) using the "User target tree" option, and then displayed with age in millions of years using Mesquite 2.75 (Maddison and Maddison, 2011). In addition, the estimates from the BEAST analyses were also summarized into a Maximum Credibility Tree in TreeAnnotator v1.5.3 (Drummond and Rambaut, 2007) using "keep target height" option, and then displayed in FigTree v1.3.1 (Rambaut, 2009). The 95% Highest Probability Density (95% HPD) values were summarized for each analysis.

3. Results

3.1. Sequence alignment

The aligned matrix with all genes combined contained 292 sequences and had 4311 sites. The 28S data had 293 sequences and the alignment resulted in 1443 sites. The Actin 5C alignment had 279 sequences and 717 sites. The 16S-ND1 alignment contained 282 sequences and 1161 sites. The COI alignment was of 190 sequences and 990 sites.

Table 1
Summary of calibration points used in divergence time analyses.

Calibration point	Analysis One	Analysis Two
Salticidae	max. 100 Ma; min. 44 Ma	max. 100 Ma; min. 44 Ma
Salticoida	max. 49 Ma; min. 16 Ma	max. 100 Ma; min. 16 Ma
Lyssomaninae/Spartaeinae	max. 100 Ma; min. 22 Ma	max. 100 Ma; min. 22 Ma
Euophryinae/Sister-group	max. 49 Ma; min. 16 Ma	max. 100 Ma; min. 16 Ma

3.2. Phylogenetic reconstruction

3.2.1. All genes combined

The results from the ML, BI and MP analyses are summarized in Fig. 1. The best tree found by ML analysis (Fig. 2) shows the monophyly of Euophryinae and of groups of euophryine genera, many of which are strongly supported by the ML bootstrap analysis (e.g. bootstrap value = 0.99 for the clade Euophryinae (node 1); 0.98 for the clade with *Variratina*, *Bulolia*, *Leptathamas* and *Coccorchestes*). *Diolenius* and its close relatives fall into a strongly supported clade (node 19, ML bootstrap value = 1.0) within the subfamily Euophryinae. However, *Bristowia* and "*Bathippus*" *pahang* Zhang, Song & Li fall outside of the Euophryinae. On the phylogeny, euophryine taxa from different continental regions tend to form their own clades with few cases of mixture (Fig. 1).

The consensus tree from the 180,000 trees retained from the two runs of the MrBayes analysis is similar to the ML tree, but with some clades collapsed. Many resolved clades have high posterior probability support values, e.g. 1.0 for Euophryinae (node 1), 1.0 for the clade with *Diolenius* and its relatives (node 19). The result of MrBayes analysis also strongly supports (posterior probability value = 1.0) the clade Saltafresia (Bodner and Maddison, 2012) including the Euophryinae as shown in the ML tree (Fig. 2). However, the placement of Euophryinae as the sister to the remaining Saltafresia is only moderately supported (posterior probability value = 0.9).

The TNT analysis was stopped after the best score was hit 10 times, and 12 equally parsimonious trees (score = 44,516) were saved. Swapping on the 12 trees in PAUP did not improve the score, but found an additional eight trees of the same score. The strict consensus tree of the 20 equally parsimonious trees is similar to the ML tree except that some of the relatively deeper branches are unresolved.

3.2.2. Individual genes

The ML tree from the 28S data (Appendix C1) recovers most of the genera or generic groups shown in the ML tree from the concatenated matrix (Figs. 1 and 2), with the exceptions of the genus *Corticattus* (JXZ305, 337), and the African euophryines with *Thyenula* spp. (JXZ103, 104, 107, 108, 149, 192) and two misplaced *Saitis* species (JXZ105, 106). However, only some of the recovered clades are well supported by the ML bootstrap analysis. The TNT analysis of 28S in combination with PAUP found 1,000,000 equally parsimonious trees (score = 11,293). The strict consensus tree of these MP trees recovers most genera and closely related genera, but many of the relatively deeper relationships are unresolved.

One species, *Athamas nitidus* (JXZ142), appears on a strikingly long branch on the ML 28S tree (Appendix C1). This suggests that a drastic shift in rates occurred on this branch, and possibly a broader shift in evolutionary model, making the placement of *Athamas* suspect (e.g., Kolaczkowski and Thornton, 2004). No 28S rDNA sequences were obtained from the other two *Athamas* species included in this study (JXZ182, 345). Preliminary analysis on the all genes data resulted in a relatively long branch for these three *Athamas* species, and placed them as a sister group of *Zabkattus*, which is not supported by morphology. The 28S data from *Athamas nitidus* (JXZ142) could be generating a misleading placement. Because of this, and because the other genes sequenced for *Athamas* tend not to show such strong phylogenetic resolution (Bodner and Maddison, 2012), we judged it safest to remove the three *Athamas* species entirely from the combined all genes

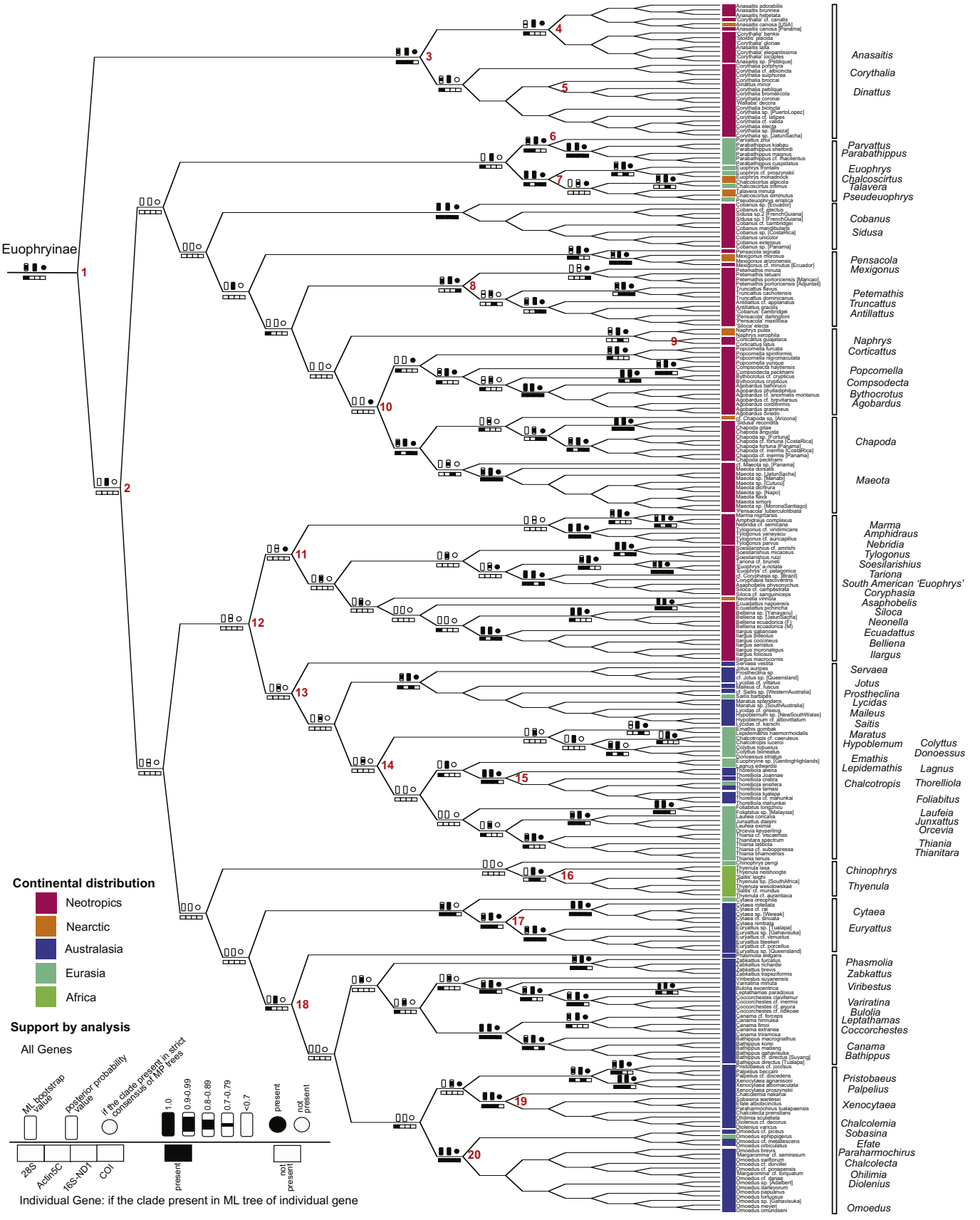

Fig. 1. Summary of phylogenetic analyses on combined matrix of all genes (28S, Actin 5C, 16S-ND1 and COI). Tree shown is the best tree from the ML analysis with all non-euophryine taxa trimmed off. Approximate position of euophryine genera is indicated on the right side of the tree; continental distribution of taxa is indicated in colored blocks in front of the taxon names. Numbers for major clades is consistent with those of Table 2.

Fig. 2. The best tree from ML analysis on combined matrix of all genes (28S, Actin 5C, 16S-ND1 and COI) with $\ln L = -181734.80$.

analyses and the dating analyses, lest their presence distort interrelationships or divergence times of other species.

Similar to 28S, most of the clades corresponding to a genus or a group of closely related genera are recognized on the ML trees from the Actin 5C matrix (Appendix C2) and the 16S-ND1 martix (Appendix C3), such as *Agobardus* spp. and the *Bathippus–Canama* clade. However, the ML bootstrap analysis shows low levels of clade support except those corresponding to closely related species. In addition, the strict consensus tree of the 1,000,000 equally parsimonious trees (score = 2687) from the Actin 5C matrix and the strict consensus tree of 46 equally parsimonious trees (score = 18,014) from the 16S-ND1 data show poor resolution at the deeper branches.

Compared to the results from other genes, the ML analysis on the COI data recovers fewer clades corresponding to genera and groups of related genera with low level of clade support from the ML bootstrap analysis (Appendix C4). The strict consensus tree of 35 equally parsimonious trees (score = 11,664) also shows little resolution.

3.3. Divergence times

A summary of the age estimates for major nodes of euophryines from the BEAST analyses under different sets of constraints is shown in Table 2. The divergence time chronogram of euophryines using the ML topology is presented in Fig. 3, with the branch length as the median age estimated from BEAST Analysis Two (with the relaxed maximum constraints on Salticoida and Euophryinae/Sister-group).

BEAST analysis with stricter maximum constraints on Salticoida and Euophryinae/Sister-group (Analysis One) indicates that the first divergence within Euophryinae (node 1) happened in the Oligocene (median = 30.19 Ma; 95% highest posterior density (HPD) = 37.84–28.93 Ma); and most of the subsequent divergences into major extant genera happened before the late Miocene (10 Ma). Loosening the maximum constraints to the nodes Salticoida and Euophryinae/Sister-group (Analysis Two) results in similar but slightly earlier median age estimate for all nodes, but the 95% HPD interval is rather wide. For instance, the median age estimate from BEAST Analysis Two for the first divergence within Euophryinae (node 1) is 33.84 Ma and the 95% HPD is 55.52–23.10 Ma. In addition, the BEAST analyses estimate the family Salticidae is about 50–60 Ma (median age estimate = 53.28 Ma from BEAST Analysis One; median age estimate = 60.03 Ma from BEAST Analysis Two).

In BEAST Analysis One, the maximum credibility tree is very similar to the ML tree from the partitioned GARLI analysis on the combined all genes matrix, except minor differences in groupings within a neotropical clade and the relative position of *Phasmolia elegans* (JXZ225) within the Papua New Guinea Clade. However, the maximum credibility tree from the BEAST Analysis Two is quite different from the ML all genes tree, and some groupings contradict the MrBayes result. For instance, the MrBayes analysis strongly supports the clade with *Parabathippus* and the Holarctic euophryines including *Euophrys*, *Talavera*, *Chalcocirtus*, *Pseudeuophrys* (posterior probability value = 1.0), whereas in the maximum credibility tree from the BEAST Analysis Two, the clade with *Parabathippus* is sister to the Neotropical *Cobanus*/*Sidusa* Clade.

In addition, the posterior probability values for some clades were lower in the BEAST analyses than in the unconstrained MrBayes analysis. For instance, the clade (node 2) with all euophryines excluding the *Anasaitis–Corythalia* Clade (node 3) has posterior probability value 0.99 from the unconstrained MrBayes analysis, but only 0.75 from the BEAST Analysis One.

4. Discussion

4.1. Phylogeny of Euophryinae

We synthesize the results from various phylogenetic analyses in Fig. 1. Although some relationships, especially those at relatively deeper levels, are still unresolved, this study provides a basic phylogenetic framework of euophryines, and resolves some clusters of euophryine genera. The phylogeny has numerous implications for euophryine taxonomy, some of which have already been implemented in taxonomic papers (Zhang and Maddison, 2012b,d), e.g. synonymizing *Pystira* and *Zenodorus* with *Omoedus* (Zhang and Maddison, 2012b). It also challenges the monophyly of some euophryine genera, such as *Chalcoscirtus*, *Corythalia*, *Euophrys* and *Thiania* (Fig. 1). However, detailed discussion of euophryine generic groups and generic delimitations is beyond the scope of this paper, and will be reviewed in an upcoming paper on euophryine genera

Table 2
Estimates of divergence times (in millions of years) for nodes in Fig. 3. Divergence times are calculated using a Bayesian relaxed molecular clock (implemented in BEAST), with two sets of constraints (Analysis One and Analysis Two; see Table 1) respectively.

#	Node name	Analysis One		Analysis Two	
		Median	95% HPD	Median	95% HPD
1	Euophryinae	30.19	[37.84, 28.93]	33.84	[55.52, 23.10]
2		29.26	[36.61, 23.19]	32.75	[53.75, 22.31]
3	*Anasaitis–Corythalia* Clade	22.27	[28.35, 16.82]	24.99	[41.39, 17.00]
4	Caribbean radiation one	19.06	[24.83, 14.20]	21.45	[35.59, 14.19]
5	Caribbean radiation two	10.35	[13.87, 7.37]	11.80	[19.63, 7.21]
6	*Parabathippus–Parvattus* Clade	20.54	[26.96, 15.16]	23.13	[38.42, 14.87]
7	*Euophrys* Clade	15.69	[20.73, 11.42]	17.39	[28.68, 11.24]
8	Caribbean radiation three	19.74	[25.49, 14.79]	22.34	[36.83, 14.77]
9	Caribbean radiation four	14.25	[19.85, 9.17]	16.44	[27.90, 9.15]
10	Caribbean radiation five	23.52	[29.70, 18.10]	26.46	[43.24, 17.75]
11		25.96	[32.94, 20.44]	29.53	[47.93, 21.22]
12		26.98	[33.96, 21.10]	30.36	[49.51, 21.68]
13		26.26	[33.14, 20.73]	29.14	[47.94, 20.02]
14		25.06	[31.60, 19.69]	27.93	[46.08, 19.15]
15	Papua New Guinea radiation one (*Thorelliola*)	16.96	[21.79, 12.68]	18.99	[31.33, 12.62]
16	African radiation	22.75	[29.50, 17.03]	25.25	[41.68, 16.51]
17	Papua New Guinea radiation two (*Cytaea–Euryattus* Clade)	16.27	[21.30, 11.79]	18.31	[30.32, 11.48]
18	Papua New Guinea radiation three	27.74	[35.09, 21.52]	31.68	[52.18, 21.65]
19	*Diolenius* Clade	19.67	[25.47, 14.73]	22.30	[36.78, 14.59]
20	*Omoedus* Clade	19.57	[25.11, 14.98]	22.04	[36.08, 14.58]

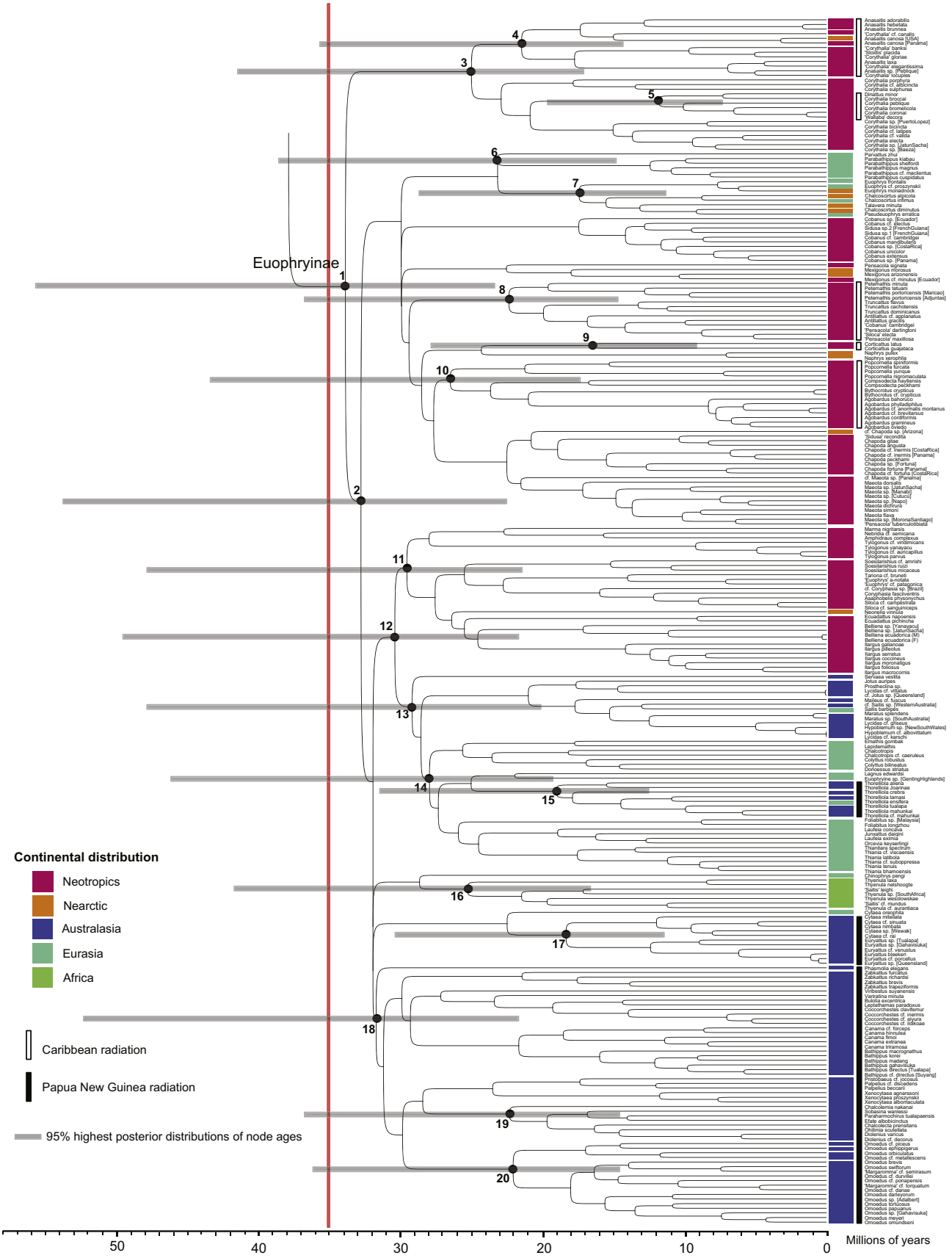

Fig. 3. Chronogram of euophryine divergence. Times shown are the median age estimates from the BEAST Analysis Two, with 95% HPD for major clades indicated as gray bars. Tree shown is the best tree from the ML analysis on all genes combined dataset with all non-euophryine taxa trimmed off. Continental distribution of taxa, and major Caribbean and Papua New Guinea Clades are indicated in front of the taxon names. Numbers for major clades are consistent with those of Table 2.

(Zhang and Maddison, unpublished). The following discussion is based mainly on the results from the ML and BI analyses.

4.1.1. Monophyly and content of Euophryinae

Previous work (Maddison and Hedin, 2003a; Maddison et al., 2008; Bodner and Maddison, 2012) supported the monophyly of Euophryinae with a small sample of euophryine genera. The monophyly of Euophryinae is further strongly supported with a dramatically extended sampling, including more than 200 species of suspected euophryines.

Maddison and Hedin (2003a) clearly indicated 34 genera as euophryines and suggested the euophryines are recognizable by typical male palp and female epigynum structures (Fig. 4A and B): the embolus is free and coiled at the distal end of the tegulum, with the plane of spiral more or less parallel to the longitudinal axis of the tegulum; the sperm duct forms a retrolateral loop projecting to the center of the tegulum; and the epigynum usually has a "window"-like structure. Almost all of their 34 genera are sampled in this study except *Ascyltus* and *Spilargis*, both of which are no doubt euophryines based on the genitalia. This study adds to these another 53 genera (see Appendix A).

4.1.2. Diolenius and its relatives are euophryines

Surprising was the placement of *Diolenius*, *Chalcolecta* and *Ohilimia* within the subfamily Euophryinae, forming a clade with *Chalcolemia*, *Efate*, *Paraharmochirus* and *Sobasina*. Although most euophryines have distinctive embolic spiral (Fig. 4A), *Diolenius* and its relatives have bizarre palpi (Fig. 4E and G), and have been placed in a separate subfamily, the Dioleniinae (Simon, 1901, 1903; Gardzińska and Żabka, 2005). Some other genera that resemble *Diolenius* in long trochanters of first legs and general body form, such as *Lystrocteisa*, *Ligonipes* and *Bristowia*, are not euophryines (also see Maddison et al., 2008).

4.1.3. "Bathippus" pahang is not a euophryine

"*Bathippus*" *pahang* was described from Malaysia (Zhang et al., 2003). Although its body form closely resembles a euophryine, the molecular phylogeny indicates that it falls outside of the euophryine clade and clusters with *Nannenus lyriger* (d105). This explains why *B. pahang* has two features that atypical for euophryines: the plane of the spiral of embolus is perpendicular to the longitudinal axis of the bulb and the tegulum lacks a retrolateral sperm duct loop.

4.2. Divergence times and biogeographical implications

Even though the present study is focused on the subfamily Euophryinae with other major salticid clades only sparsely sampled, it obtained similar age estimates for the family Salticidae and its main groups as the previous study by Bodner and Maddison (2012). Implications of divergence time estimates on the historical biogeography of Euophryinae are discussed below.

4.2.1. Continental biogeography

Similar to findings in other salticid lineages (Maddison and Hedin, 2003a; Maddison et al., 2008; Bodner and Maddison, 2012), the reconstructed phylogeny shows that the Old World and New World euophryines are usually grouped in their own clades with very few cases of intercontinental mixing—most divergences within Euophryinae appear to be intracontinental (see coloring in Fig. 1). This pattern suggests most diversification within the Euophryinae happened in the Cenozoic after the New and Old World continents were isolated; otherwise, we would expect that taxa with Old World and New World distributions would be more mixed on the phylogeny.

Euophryines are most diverse in the Neotropical and Australasian regions. This might suggest they have a Gondwanaland origin (Hill, 2009). Australia and South America remained in contact

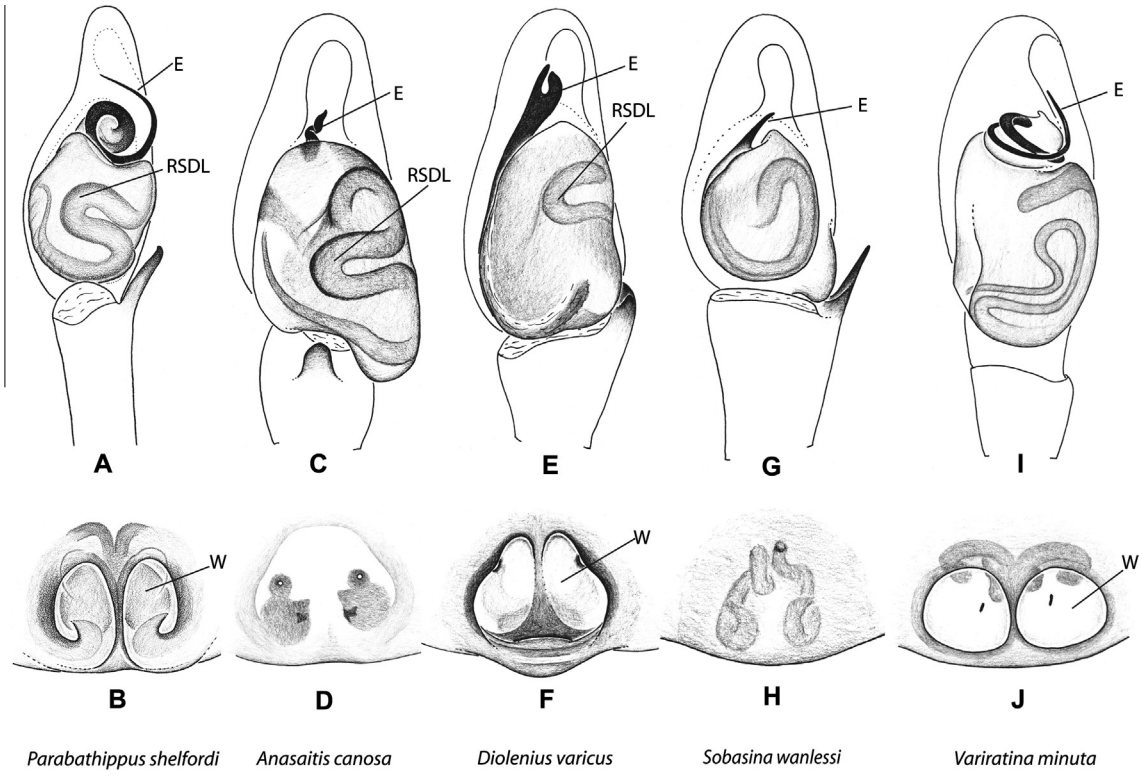

Fig. 4. Examples of male palp (A, C, E, G, and I) and female epigynum (B, D, F, H, and J) strucures of euophryine jumping spiders. (A and B) *Parabathippus shelfordi*; (C and D) *Anasaitis canosa*; (E and F) *Diolenius varicus*; (G and H) *Sobasina wanlessi*; (I and J) *Variratina minuta*. Abbreviations: E, embolus; RSDL, retrolateral sperm duct loop; W, window of epigynum. Figures (G–J) are from Zhang and Maddison (2012b).

through an Antarctic land bridge until the end of the Eocene (35 Ma) (Sanmartín and Ronquist, 2004). The BEAST analyses result in a wide range of 95% HPD for the very early divergence of euophryines with the upper boundary earlier than 35 Ma. This indicates euophryines may be old enough for the southern Gondwanaland origin, and the Antarctic land bridge could have played an important role in facilitating the faunal exchange between southern South America and Australia in the early evolutionary history of euophryines.

However, if euophryines used the Antarctic land bridge early in their history to cross between South America and Australasia, why did other major salticoid clades in those continents and of about the same age not successfully cross Antarctica and diversify in both hemispheres? Two major salticoid clades, Amycoida (mostly in the Neotropics) and Astioida (mainly in Australasia), are highly diversified in one of these two regions but have very few (apparently recently dispersed) representatives in the other. According to Bodner and Maddison (2012), the Amycoida (32–39 Ma) and Astioida (31–39 Ma) are about as old as Euophryinae. Could the euophryines have crossed Antarctica but the amycoids and astioids failed?

At the dated time of the early diversification of euophryines, a significant worldwide temperature decline led to a switch from a "greenhouse" to an "icehouse" world, and probably also caused a dramatic faunal turnover on the earth with warm tropical taxa being replaced by cooler temperate taxa (Zanazzi et al., 2007; Hines, 2008). This implies that euophryines would have needed cold tolerance if they were to have crossed through the polar Antarctica. There are hints that extant euophryines may in fact be especially cold tolerant. First, even though euophryines and amycoids are found throughout most of South America, amycoids tend to dominate diversity at lower elevations, euophryines at higher elevations (Maddison, personal observation). Second, by far the most common jumping spiders in cold and wet areas of southern South America are a group of euophryines described as "*Euophrys*" (e.g. "*Euophrys*" *a-notata*, "*Euophrys*" *patagonica*, "*Euophrys*" *tehuelche*, etc.). Tolerance to low temperature may have facilitated euophryines in particular to cross Antarctica after the late Eocene when the temperature dramatically dropped in this continent.

Even if vicariance during the south Gondwana breakup explains some early euophryine divergences, dispersal must have played an important role later in the historical biogeography of euophryines, because several clades with mixed euophryine lineages from different continents are younger than the continental splits (Fig. 3). For instance, there are apparent dispersals across Wallace's line between Australasia and Eurasia (ca. 10–23 Ma; see genera such as *Thiania*, *Saitis*, *Thorelliola*, *Cytaea*, and *Euryattus*). Dispersals between North America and Eurasia are most likely through the Bering land bridge (ca. 5–10 Ma; Sanmartín et al., 2001; see genera *Euophrys*, *Chalcoscirtus*, *Talavera* and *Pseudeuophrys*). The faunal exchange between the Neotropic and Nearctic regions (ca. 3–26 Ma; see genera *Anasaitis*, *Naphrys*, *Mexigonus* and *Neonella*) was possibly through the rows of islands in the Caribbean Sea and the Panama Island Arc, and later via the Isthmus of Panama (Sanmartín and Ronquist, 2004; Iturralde-Vinent, 2006).

4.2.2. Two "hot-spots" of euophryine diversity

Euophryines have developed two independent "hot spots" of diversity: New Guinea (Old World) and the Caribbean Islands (New World). Euophryine spiders are more dominant in both species diversity and abundance in the jumping spider community of these two regions compared to any other areas in the Neotropics and Asian tropics (also see Maddison and Zhang, 2011). For example, during a jumping spider expedition to the Dominican Republic and Puerto Rico in 2009, at least 80% of salticid species and specimens collected were euophryines.

Most euophryines from New Guinea fall into one clade and represent a single radiation (Fig. 3, node 18), with the only exceptions being the *Cytaea–Euryattus* Clade (node 17) and the *Thorelliola* Clade (node 15). The large New Guinea clade contains the most diverse body forms of euophryines. Some body forms, such as the ant-like form (*Sobasina* and *Paraharmochirus*), the beetle-like form (*Coccorchestes*), and the weird forms of *Diolenius* and *Leptathamas*, are not found anywhere else in the world but New Guinea (Fig. 5). The age for this radiation is estimated as 27–32 Ma, which implies euophryines were probably among the earliest salticoid immigrants in New Guinea and explains why they are so abundant in the local salticid community. The other two euophryine clades that are also well-known from New Guinea, *Thorelliola* and *Cytaea/Euryattus*, are much younger (16–19 Ma), and they seem to represent independent radiations later into New Guinea.

In contrast, the Caribbean euophryines are embedded within two big clades, and seem to represent as many as five independent radiations, most likely from South America (Fig. 3). These radiations are dated from the late Eocene to the middle Miocene (ca. 40–10 Ma) when various rows of islands existed in the Caribbean Sea (Iturralde-Vinent, 2006). Euophryines in the Caribbean Islands have all the body forms that appear in the other areas of Neotropics. However, the body form diversity from this region is not comparable to that of New Guinea.

4.3. Other implications from the molecular phylogeny

Although most of the genera determined to be within the Euophryinae have a typical palp and epigynum as described above (and Maddison and Hedin, 2003a; Fig. 4A and B), some of them have other forms of genitalia. For instance, the embolus of *Diolenius* comes from the proximal end of the bulb instead of the distal end (Fig. 4E); the sperm duct of *Sobasina* does not form the retrolateral loop (Fig. 4G); the plane of the embolic spiral of *Variratina* is perpendicular to the longitudinal axis of the tegulum rather than parallel (Fig. 4I); *Sobasina* and *Tylogonus* have fixed embolus; *Anasaitis* has no obvious window in the epigynum (Fig. 4D). However, these genera are closely related to others with typical euophryine-like genitalia, or clearly derived from within a clade with typical genitalia. This indicates that these abnormal genitalic forms are derived from the typical euophryine-like genitalic structures.

Myrmecophagy (ant-eating) is relatively rare in jumping spiders probably due to the ants' defenses of powerful mandibles, poison-injecting sting and formic acid (Jackson and Li, 2001). However, some salticid species routinely feed on ants using ant-specific prey-capture tactics. Among more than 20 salticids that have been thoroughly studied and appear to be ant-feeding specialists, about half of them are euophryines: *Chalcotropis* (six species), *Xenocytaea* (two species), *Zenodorus* (=*Omoedus*, three species), *Anasaitis* (one species), *Naphrys* (one species) (Jackson et al., 1998; Clark et al., 2000; Jackson and Li, 2001). The scattered placement of these lineages on the phylogeny seems to suggest the myrmecophagic behavior may have evolved not only independently in the Old World and the New World, but also separately in different lineages in each continent. However, more ecological data on whether or not other euophryines are ant-feeding specialists are needed to understand the evolution of myrmecophagy in Euophryinae.

Within the big New Guinea radiation (node 18), the *Diolenius*-Clade (node 19) contains species that resemble ants (e.g. *Sobasina* and *Paraharmochirus*), and the *Omoedus*-Clade (node 20) has members specialized in ant-feeding (e.g. *Omoedus durvillei* (Walckenaer), see Jackson and Li, 2001 as *Zenodorus durvillei*). An interesting finding from this study is that these two lineages are both about 19–22 Ma. Their similarity in age implies that their ancestors followed two completely different evolutionary paths

Fig. 5. Examples of body forms of euophryine jumping spiders, with (A–F) show typical euophryine body forms and (G–L) show the diverse body forms of euophryines in New Guinea. (A) *Corythalia bicincta* (female); (B) *Euophrys frontalis* (male); (C) *Ecuadattus typicus* (male); (D) *Popcornella spiniformis* (male); (E) *Colyttus striatus* (female); (F) *Cobanus cambridgei* (Bryant) (male); (G) *Omoedus papuanus* (male); (H) *Coccorchestes* cf. *aiyura* (male); (I) *Leptathamas paradoxus* (male); (J) *Diolenius varicus* (male); (K) *Chalcolecta prensitans* (female); (L) *Paraharmochirus tualapaensis* (male). Figure (G) is copyright © 2012 W.P. Maddison, (A–F, H–L) are copyright © 2013 W.P. Maddison, released under a Creative Commons Attribution (CC-BY) 3.0 license.

after encountering ants: one went for ant-mimicry, and the other for ant-eating.

Acknowledgments

This work was funded by an NSERC Canada Discovery Grant to W.P.M. We would like to thank people who generously loaned us specimens in museums or private collections for molecular studies, without which this study would have been impossible: Dr. Charles Griswold, Dr. G.B. Edwards, Dr. Gustavo R.S. Ruiz, Dr. Alexander Riedel, Dr. Marek Zakba, Dr. Rosemary G. Gillespie, Dr. Damian O. Elias, Mr. Ken Schneider. Acknowledgements are due to Dr. Stephen Richards, Mr. J. Brocca, Dr. Ingi Agnarsson, Dr. D. Li, Prof. Mingsheng Zhu, Dr. Michael L. Draney and Dr. Petra Sierwald for their effort in organizing field trips during which some specimens used in this study were collected. Additional assistance in the field was also provided by N. Corona, J. Brocca, G.B. Edwards, Gustavo R.S. Ruiz, Bruce Beehler, Modi Pontio, Victoria Niesi, William H. Thomas, Max Kuduk, Muse Opiang, Banak Gamui, Jim Robins, Ingi Agnarsson, Jeremy Woon, W.G. Lian and H.Q. Ma. We also would like to express our gratitude to Dr. Charles Griswold for constructive feedback on this work; to Dr. Marshal C. Hedin for suggestions on divergence time analyses; and to Melissa R. Bodner for her assistance in some molecular work.

Appendix A. Supplementary material

Supplementary data associated with this article can be found, in the online version, at http://dx.doi.org/10.1016/j.ympev.2013.03.017.

References

Altekar, G., Dwarkadas, S., Huelsenbeck, J.P., Ronquist, F., 2004. Parallel Metropolis-coupled Markov chain Monte Carlo for Bayesian phylogenetic inference. Bioinformatics 20, 407–415.

Bodner, G.S.S., 2002. Biodiversity Assessment and Systematics of Neotropical Jumping Spiders (Araneae: Salticidae). PhD Thesis, 450pp.

Bodner, M.R., Maddison, W.P., 2012. The biogeography and age of salticid spider radiations (Araneae: Salticidae). Molecular Phylogenetics and Evolution 65, 213–240.
Clark, R.J., Jackson, R.R., Culter, B., 2000. Chemical cues from ants influence predatory behavior in *Habrocestum pulex*, and ant-eating jumping spider (Araneae, Salticidae). The Journal of Arachnology 28, 309–318.
Drummond, A.J., Rambaut, A., 2007. BEAST: Bayesian evolutionary analysis by sampling trees. BMC Evolutionary Biology 7, 214.
Ewing, B., Green, P., 1998. Basecalling of automated sequencer traces using phred. II. Error probabilities. Genome Research 8, 186–194.
Ewing, B., Hillier, L., Wendl, M., Green, P., 1998. Basecalling of automated sequencer traces using phred. I. Accuracy assessment. Genome Research 8, 175–185.
Gardzińska, J., Żabka, M., 2005. A revision of the spider genus *Chalcolecta* Simon, 1884 (Araneae: Salticidae). Annales Zoologici Warszawa 55, 437–448.
Goloboff, P.A., Farris, J.S., Nixon, K.C., 2008. TNT, a free program for phylogenetic analysis. Cladistics 24 (5), 774–786.
Green, P., 1999. Phrap, Version 0.990329. Distributed by the Author. <http://www.phrap.org>.
Green, P., Ewing, B., 2002. Phred, Version 0.020425 c. Distributed by the Authors. <http://phrap.org>.
Hedin, M.C., 1997. Molecular phylogenetics at the population/species interface in cave spiders of the southern Appalachians (Araneae: Nesticidae: Nesticus). Molecular Biology and Evolution 14, 309–324.
Hedin, M.C., Maddison, W.P., 2001. A combined molecular approach to phylogeny of the jumping spider family Dendryphantinae (Araneae: Salticidae). Molecular Phylogenetics and Evolution 18 (3), 386–403.
Hill, D.E., 2009. Salticidae of the Antarctic land bridge. Peckhamia 76 (1), 1–14.
Hines, H.M., 2008. Historical biogeography, divergence time, and diversification patterns of bumble bees (Hymenoptera: Apidae: *Bombus*). Systematic Biology 57 (1), 58–75.
Huelsenbeck, J.P., Ronquist, F., 2001. MrBayes: Bayesian inference of phylogenetic trees. Bioinformatics 17, 754–755.
Iturralde-Vinent, M.A., 2006. Meso-Cenozoic Caribbean paleogeography: implications for the historical biogeography of the region. International Geology Review 48, 791–827.
Jackson, R.R., Li, D., 2001. Prey-capture techniques and prey preferences of *Zenodorus durvillei*, *Z. metallescens* and *Z. orbiculatus*, tropical ant-eating jumping spiders (Araneae: Salticidae) from Australia. New Zealand Journal of Zoology 28, 299–341.
Jackson, R.R., Li, D., Barrion, A.T., Edwards, G.B., 1998. Prey-capture techniques and prey preferences of nine species of ant-eating jumping spiders (Araneae: Salticidae) from the Philippines. New Zealand of Zoology 25, 249–272.
Kolaczkowski, B., Thornton, J.W., 2004. Performance of maximum parsimony and likelihood phylogenetics when evolution is heterogeneous. Nature 431, 980–984.
Larkin, M.A., Blackshields, G., Brown, N.P., Chenna, R., McGettigan, P.A., McWilliam, H., Valentin, F., Wallace, I.M., Wilm, A., Lopez, R., Thompson, J.D., Gibson, T.J., Higgins, D.G., 2007. Clustal W and Clustal X version 2.0. Bioinformatics 23 (21), 2947–2948.
Maddison, W.P., Bodner, M.R., Needham, K.M., 2008. Salticid spider phylogeny revisited, with the discovery of a large Australasian clade (Araneae: Salticidae). Zootaxa 1893, 46–64.
Maddison, W.P., Hedin, M.C., 2003a. Jumping spider phylogeny (Araneae: Salticidae). Invertebrate Systematics 17, 529–549.
Maddison, W.P., Hedin, M.C., 2003b. Phylogeny of *Habronattus* jumping spiders (Araneae: Salticidae), with consideration of genital and courtship evolution. Systematic Entomology 28, 1–21.
Maddison, W.P., Maddison, D.R., 2010a. Mesquite: A Modular System for Evolutionary Analysis. Version 2.73. <http://mesquiteproject.org>.
Maddison, D.R., Maddison, W.P., 2010b. Chromaseq: A Mesquite Module for Analyzing Sequence Chromatograms. Version 0.984. <http://mesquiteproject.org/packages/chromaseq>.
Maddison, W.P., Maddison, D.R., 2011. Mesquite: A Modular System for Evolutionary Analysis. Version 2.75. <http://mesquiteproject.org>.
Maddison, W.P., Needham, K.M., 2006. Lapsiines and hisponines as phylogenetically basal salticid spiders (Araneae: Salticidae). Zootaxa 1255, 37–55.
Maddison, W.P., Zhang, J., 2011. Salticid spiders of Papua New Guinea. In: Richards, S.J., Gamui, B.G. (Eds.), Rapid Biological Assessments of the Nakanai Mountains and the Upper Strickland Basin: Surveying the Biodiversity of Papua New Guinea's Sublime Karst Environments. RAP Bulletin of Biological Assessment 60. Conservation International, Arlington, VA, pp. 186–189 (Chapter 14).
Maddison, W.P., Zhang, J., Bodner, M.R., 2007. A basal phylogenetic placement for the salticid spider *Eupoa*, with descriptions of two new species (Araneae: Salticidae). Zootaxa 1432, 23–33.
Masta, S.E., Boore, J.L., 2004. The complete mitochondrial genome sequence of the spider *Habronattus oregonensis* reveals rearranged and extremely truncated tRNAs. Molecular Biology and Evolution 21 (5), 893–902.
Penney, D., 2008. Dominican Amber Spiders: A Comparative Palaeontological–Neontological Approach to Identification, Faunistics, Ecology and Biogeography. Siri Scientific Press.
Platnick, N.I., 2012. The World Spider Catalog, Version 13.0. American Museum of Natural History. <http://research.amnh.org/iz/spiders/catalog>.
Posada, D., Buckley, T.R., 2004. Model selection and model averaging in phylogenetics: advantages of the AIC and Bayesian approaches over likelihood ratio tests. Systematic Biology 53, 793–808.
Posada, D., Crandall, K.A., 1998. Modeltest: testing the model of DNA substitution. Bioinformatics 14 (9), 817–818.
Prószyński, J., 1976. Studium systematyczno-zoogeograficzne nad rodziną Salticidae (Aranei) Regionów Palearktycznego i Nearktycznego. Wyższa Szkoła Pedagogiczna w Siedlcach 6, 1–260.
Rambaut, A., 2009. Tree Figure Drawing Tool. Version 1.3.1. Institute of Evolutionary Biology, University of Edinburgh. <http://tree.bio.ed.ac.uk/software/figtree/>.
Rambaut, A., Drummond, A.J., 2007. Tracer v1.4. <http://beast.bio.ed.ac.uk/Tracer>.
Ronquist, F., Huelsenbeck, J.P., 2003. MRBAYES 3: Bayesian phylogenetic inference under mixed models. Bioinformatics 19, 1572–1574.
Sanmartín, I., Enghoff, H., Ronquist, F., 2001. Patterns of animal dispersal, vicariance and diversification in the Holarctic. Biological Journal of the Linnean Society 73, 345–390.
Sanmartín, I., Ronquist, F., 2004. Southern hemisphere biogeography inferred by event-based models: plant versus animal patterns. Systematic Biology 53 (2), 216–243.
Simon, C., Franti, F., Beckenbach, A., Crespi, B., Liu, H., Flook, P., 1994. Evolution, weighting and phylogenetic utility of mitochondrial gene sequences and a compilation of conserved polymerase chain reaction primers. Annals of the Entomological Society of America 87, 651–701.
Simon, E., 1901. Histoire naturelle des araignées. Paris 2, 381–668.
Simon, E., 1903. Histoire naturelle des araignées. Paris 2, 669–1080.
Stamatakis, A., 2006. RAxML-VI-HPC: maximum likelihood-based phylogenetic analyses with thousands of taxa and mixed models. Bioinformatics 22 (21), 2688–2690.
Stamatakis, A., Hoover, P., Rougemont, J., 2008. A rapid bootstrap algorithm for the RAxML web servers. Systematic Biology 57 (5), 758–771.
Swofford, D.L., 2002. PAUP*. Phylogenetic Analysis Using Parisomny (*and Other Methods). Version 4.0b10. Sinauer Associates, Sunderland, Massachusetts, USA.
van der Auwera, G., Chapelle, S., de Wachter, R., 1994. Structure of the large ribosomal subunit RNA of *Phytophthora megasperma*, and phylogeny of the oomycetes. Federation of European Biochemical Societies Letters 338, 133–136.
Vink, C.J., Hedin, M.C., Bodner, M.R., Maddison, W.P., Hayashi, C.Y., Garb, J.E., 2008. Actin 5C, a promising nuclear gene for spider phylogenetics. Molecular Phylogenetics and Evolution 48 (1), 377–382.
Weitschat, W., Wichard, W., 2002. Atlas of plants and animals in Baltic amber. Geological Magazine 139 (5), 597.
Wheeler, W.C., Gatesy, J., DeSalle, R., 1995. Elision: a method for accommodating multiple molecular sequence alignments with alignment-ambiguous sites. Molecular Phylogenetics and Evolution 4, 1–9.
Wheeler, T.J., Kececioglu, J.D., 2007. Multiple alignments by aligning alignments. Bioinformatics 23, 559–568.
Zanazzi, A., Kohn, M.J., MacFadden, B.J., Terry, D.O., 2007. Large temperature drop across the Eocene–Oligocene transition in central North America. Nature 445, 639–642.
Zhang, J., Maddison, W.P., 2012a. New euophryine jumping spiders from the Dominican Republic and Puerto Rico (Araneae: Salticidae: Euophryinae). Zootaxa 3476, 1–54.
Zhang, J., Maddison, W.P., 2012b. New euophryine jumping spiders from Papua New Guinea (Araneae: Salticidae: Euophryinae). Zootaxa 3491, 1–74.
Zhang, J., Maddison, W.P., 2012c. New euophryine jumping spiders from Central America and South America (Araneae: Salticidae: Euophryinae). Zootaxa 3578, 1–35.
Zhang, J., Maddison, W.P., 2012d. New euophryine jumping spiders from Southeast Asia and Africa (Araneae: Salticidae: Euophryinae). Zootaxa 3581, 53–80.
Zhang, J., Song, D.X., Li, D., 2003. Six new and one newly recorded species of Salticidae (Arachnida: Araneae) from Singapore and Malaysia. The Raffles Bulletin of Zoology 51, 187–195.
Zwickl, D.J., 2006. Genetic Algorithm Approaches for the Phylogenetic Analysis of Large Biological Sequence Datasets under the Maximum Likelihood Criterion. PhD Dissertation. The University of Texas at Austin.